Title

Interaction of Group IA Phospholipase A2 with Metal Ions and Phospholipid Vesicles Probed with Deuterium Exchange Mass Spectrometry

Journal

Biochemistry, 47(24)

ISSN

0006-2960

Authors

Burke, John E
Karbarz, Mark J
Deems, Raymond A
et al.

Publication Date

2008-06-01

DOI

10.1021/bi8000962

Peer reviewed

Published in final edited form as:
Biochemistry. 2008 June 17; 47(24): 6451–6459.

Interaction of Group IA Phospholipase A_2 with Metal Ions and Phospholipid Vesicles Probed with Deuterium Exchange Mass Spectrometry

John E. Burke[#], **Mark J. Karbarz**[#], **Raymond A. Deems**[#], **Sheng Li**[‡], **Virgil L. Woods Jr.**[‡,*], and **Edward A. Dennis**[#,*]

#Department of Chemistry and Biochemistry and Department of Pharmacology, School of Medicine, University of California, San Diego, La Jolla, California 92093-0601

‡*Department of Medicine and Biomedical Science Graduate Program, School of Medicine, University of California, San Diego, La Jolla, California 92093-0601*

Abstract

Deuterium exchange mass spectrometric evaluation of the cobra venom (*Naja naja naja)* Group IA phospholipase A_2 (GIA PLA_2) was carried out in the presence of the metal ions Ca^{2+} and Ba^{2+} and phospholipid vesicles. Novel conditions for digesting highly disulfide bonded proteins and a methodology for studying protein-lipid interactions using deuterium exchange have been developed. The enzyme shows unexpectedly slow rates of exchange in the two large alpha helices at regions 43-53 and 89-101, which suggests that these alpha helices are highly rigidified by the four-disulfide bonds in this region. The binding of Ca^{2+} or Ba^{2+} ions decreased the deuterium exchange rates for five regions of the protein (24-27, 29-40, 43-53, 103-110, and 111-114). The magnitude of the changes was the same for both ions with the exception of regions 24-27 and 103-110 which showed greater changes for Ca^{2+}. The crystal structure of the *N. naja naja* GIA PLA_2 contains a single Ca^{2+} bound in the catalytic site, but the crystal structures of related PLA_2s contain a second Ca^{2+} binding site. The deuterium exchange studies reported here clearly show that in solution the GIA PLA_2 does in fact bind two Ca^{2+} ions. With dimyristoyl phosphatidylcholine (DMPC) phospholipid vesicles with 100 μM Ca^{2+} present at 0 °C, significant areas on the i-face of the enzyme showed decreases in exchange. These areas included regions 3-8, 18-21, and 56-64 which include Tyr-3, Trp-61, Tyr-63, and Phe-64 proposed to penetrate the membrane surface. These regions also contained Phe-5, and Trp-19, proposed to bind the fatty acyl tails of substrate.

The phospholipase A_2 (PLA_2) superfamily consists of fifteen different groups and many subgroups that hydrolyze the ester bond of 2-acyl fatty acids from phospholipids (1,2). The products of this reaction, free fatty acids and lysophospholipids, play many different roles as second messengers and precursors for important bioactive molecules (3). One of the best studied PLA_2 enzymes is the cobra (*Naja naja naja)* venom Group IA (GIA) PLA_2. This is one of the secreted PLA_2s that are characterized by their low molecular weight, Ca^{2+} requirement for catalysis, and the presence of seven disulfide bonds. This enzyme is able to hydrolyze monomeric phospholipid substrates, but there is a substantial increase in activity when the enzyme acts on large lipid aggregates (4). This enzyme has also been shown to be activated by phospholipids containing phosphatidylcholine head groups (5), and two possible sites for this interaction have been suggested (6,7). Site-directed mutagenesis identified an activator site distinct from the catalytic site (8). Extensive kinetic and biophysical studies have

*Corresponding authors. EAD: Phone, 858-534-3055; FAX, 858-534-7390; E-mail, edennis@ucsd.edu; VLW: Phone, 858-534-2180; FAX, 858-534-2606; E-mail, vwoods@ucsd.edu.

been done to understand how soluble enzymes interact with lipid interfaces and to define how the interface affects enzyme kinetics. Many of these studies were carried out on the GI and GII PLA_2s. Thus, the cobra venom GIA PLA_2 has been an important model of not only phospholipid metabolism, but for all of lipid enzymology as well (9).

Biophysical studies on lipid metabolizing enzymes acting on phospholipids are complicated because this system involves two large macromolecules, the enzyme and the aggregated phospholipid vesicle. The size of the lipid aggregates present limitations for many standard biophysical techniques such as solution NMR and X-ray crystallography. For example, many X-ray crystal studies of the secreted PLA_2s have been conducted including two of the GIA *N. naja naja* enzyme (6,10). These studies were carried out in the presence of metal ions, but not in the presence of large lipid aggregates. Crystallography reports only the state of the enzyme in a crystal not its state in solution, yet the solution dynamics of the interactions between the PLA_2 and the interface may affect enzyme activity. The N. naja naja enzyme has also been studied with NMR in the presence of a monomeric small lipid inhibitor, and a micellar phospholipid analogue (11,12), but no studies have been reported with natural phospholipids. In an attempt to utilize a technique that can yield both structural information in solution and information about the dynamics of the enzyme-phospholipid surface interaction, we have employed deuterium exchange mass spectrometry to study PLA_2 lipid/surface interactions and used this technique to add valuable information about these processes.

Peptide amide hydrogen/deuterium exchange analyzed via liquid chromatography/mass spectrometry (DXMS) has been widely used to analyze protein-protein interactions (13,14), protein conformational changes (15,16), protein dynamics (17), and protein-lipid interactions (18) on proteins lacking disulfide bonds. Tris-carboxy ethyl phosphine (TCEP) has regularly been used to reduce proteins containing one or two disulfide bonds, and occasionally more (19). However, denaturing and reducing as highly a disulfide bonded protein as the GIA PLA_2 which contains 14 cysteines, all in disulfide bonds, out of 119 amino acids is extremely challenging and not previously reported using the DXMS technique. We have now employed DXMS to examine the effects of metal ion binding on solvent accessibility and protein structure. We have probed the structural dynamics of the protein and found large changes in accessibility of the amide hydrogens in heavily disulfide bonded regions of the protein. We have also confirmed the presence of the primary Ca^{2+} -binding site and a secondary Ca^{2+} -binding site. We have also studied the interactions of the soluble GIA PLA_2 with a lipid surface and found a deuterium exchange difference on the interfacial side of the enzyme in the presence of phospholipid vesicles. This has advanced our understanding of the structure and dynamics of the secreted PLA_2's in solution.

Materials and Methods

Materials

Cobra venom PLA_2 was purified as described previously (20) and stored at −20 °C in 10 mM Tris pH 7.5. Phospholipids were purchased from Avanti Polar Lipids. All other reagents are analytical reagent grade or better.

On Exchange

D_2O buffer contains 10 mM Tris (pH 7.5), 50 mM NaCl, (+/-)1mM $CaCl_2$ or $BaCl_2$ in 98% D_2O. Hydrogen/Deuterium exchange experiments were initiated by mixing 10 μl of 10 mM Tris pH (7.5) containing 40 μg of GIA PLA_2 with 30 μl of D_2O buffer producing a final D_2O concentration of 74% at pH 7.5. In the experiments examining metal ion binding, the GIA PLA_2 was pre-incubated with 4 mM $BaCl_2$ or $CaCl_2$ at 22 °C for 5 min. The optimized temperature for separating both fast and slow exchanging regions was 22 °C.

The H/D exchange samples were incubated in 22°C for 15 s, 60 s, 600 s, 3600 s, and 14,400 s at pH 7.5. This gave the greatest distribution of deuterium incorporation over our time course. For the phospholipid experiments, the last time point was dropped. Each time point was repeated three times. The deuterium exchange was quenched by adding 160 μl ice-cold quench solution (8 M GdHCl, 1 M TCEP) buffered with formic acid to a pH of 2.5. The samples were placed on ice for 15 min.

Full Exchange

A fully deuterated sample was prepared by adding GIA PLA_2 to a solution of 8 M GdHCl and 1 M TCEP dissolved in 100% D_2O and allowing this to stand at room temperature for 24 hrs. The GdHCl and TCEP were removed by diluting the solution with 1 volume of 100% D_2O and concentrating the protein with an Amicon Ultra 5000 MW cutoff centrifuge filter (Millipore) at 3000g until the volume was half of the original volume. This was repeated 10 times to remove all TCEP and GdHCl. The protein was allowed to sit for 2 hrs after removal of all denaturants and was then digested under normal conditions.

Off Line Protein Digestion

To adequately digest the GIA PLA_2, an off line digestion step had to be added in front of the digestion that occurs during the automated process outlined below. The quenched protein solutions containing 40 μg of protein were added to a 50 μl slurry of ice cold immobilized pepsin (Pierce Biotechnology) and fungal XIII proteases immobilized on 6% cross linked agarose beads suspended in 0.8% formic acid and allowed to sit for 15 min. Immobilized fungal XIII protease was prepared as described previously (16). This solution was placed in a 5 Micron ultrafree-MC centrifugal filter (Millipore) and centrifuged at 700 G (eppendorf centrifuge 5415C) to remove the immobilized proteases and the remaining solution was frozen on dry ice to stop all further amide hydrogen exchange.

Automated Proteolysis-liquid-chromatography-mass spectrometry analysis of samples

Samples were then loaded onto the automated DXMS system (14) that digested the proteins, separates the peptides and performs the mass spec analysis. All steps were performed at 0 °C as previously described (14,16). The samples were hand-thawed on melting ice and injected onto a protease column (66 μl bed volume) containing porcine pepsin (Sigma; immobilized on Poros 2 AL medium at 30 mg/ml following the manufacturer's instructions, Applied Biosystems), at a flow rate of 100 ul/min with 0.05% (v/v) trifluoracetic acid (TFA). The eluate from the pepsin column flowed directly onto a C18 column 50 mM length 1.0 mM ID (Vydac cat #218MS5150). The peptides were eluted with a linear gradient from 0.046% TFA, 6.4% (v/v) acetonitrile to 0.03% TFA, 38.4% acetonitrile at 50 ul/min. The C18 column eluate flowed directly into a Finnigan LCQ Classic mass spectrometer via its ESI probe operated with a capillary temperature of 200°C as previously described (14,16).

The presence of large amounts of phospholipid in peptide eluates injected into the mass spectrometer would significantly degrade the peptide analysis. We found that the C-18 column employed in the peptide separation bound all of the phospholipids that were carried through the workup in the phospholipid binding experiments. Thus, no extra steps were required to remove it. Up to ten runs could be completed before the phospholipid bound to the columns began to degrade the peptide separation or yields. After every ten runs the HPLC column was flushed with 100% methanol for 30 minutes to remove the bound phospholipids.

Lipid preparation and on exchange

Lipid vesicles were prepared by adding the lipid in chloroform to a small glass tube and evaporating the solvent under argon. The lipid was resuspended in 100 mM KCl at 40 mM and

allowed to sit at 50 °C for 30 min. This solution was then bath sonicated for 10 min. This solution was then size excluded using 10 passes over a mini extruder (Avanti Polar Lipids) with a 0.03 μM polycarbonate membrane. For lipid binding studies, the enzyme was studied with two different lipid systems dipalmitoyl phosphatidylcholine (DPPC) and dimyristoyl phosphatidylcholine (DMPC) and they were used to study lipid binding at 22 °C and 0 °C, respectively. Experiments were performed on the gel state of the lipid to prevent excess activity and to prevent the lag phase in activity associated with lipids above the phase transition temperature (26). For DPPC experiments, the enzyme was pre-incubated with 4 mM DPPC SUVs at 22 °C for 5 min plus the addition of either 4 mM $BaCl_2$ or 4 mM EDTA. This gave a total concentration after addition of deuterium of 1 mM DPPC and 1 mM $BaCl_2$ or EDTA.

For DMPC experiments, the enzyme was preincubated with 4 mM DMPC SUVs at 0°C in the presence of 100 μM Ca^{2+} to minimally activate the enzyme. A modified version of the Dole assay (8) using the exact same conditions as used for deuterium exchange experiments was used to assay enzyme activity. Deuterium exchange results were only obtained for timepoints with less then 10% hydrolysis of lipid vesicles to prevent acidification of exchange buffer, and effects of non phospholipid lipid aggregates. The enzyme was pre-incubated with 4 mM DMPC lipid vesicles with 400 μM Ca^{2+} for 30 seconds at 0 °C. This gave a total concentration after dilution by the addition of deuterated buffer of 1 mM DMPC and 100 μM Ca^{2+}. The K_d of the enzyme for lipid vesicles at 40 °C is 4.4 mM, but lipid concentrations over 1 mM were limited by the amount of protein required for mass spectrometry analysis. The mole ratio of lipid molecules to protein molecules in the samples was ~16:1.

Data processing

SEQUEST (Thermo Finnigan Inc.) was used to assign peptide sequences to the ions peaks eluting from the C-18 column from their ms/ms spectra. Peaks that SEQUEST identified where then analyzed with DXMS Explorer (Sierra Analytica Inc, Modesto CA) as previously described (14,16). All peptides selected for analysis had to first pass the quality-control thresholds setup in the DXMS software and then were manually checked. If the same peptide was found with different charges (1, 2 or 3), the one with the best signal/noise ratio was selected for analysis. The mass of the peptide was determined by measuring the centroid of the isotopic envelope of the peptide. The level of deuterium on a given peptide is expressed as the incorporated deuteron number (Inc#). The incorporated deuteron number is the difference between the centroids of a given peptide in non-deuterated and deuterated samples. Back-exchange was ~35-50% due to the long digestion time but was corrected using the fully deuterated control experiments. The deuteration level (D) is the ratio of the Inc# of the sample to the Inc# of a fully deuterated sample given by the following equation (21).

$$D = \left[\frac{m_s - m_{0\%}}{m_{100\%} - m_{0\%}} \right] N$$

Where m_i is the centroid of the peptide exposed to s = sample conditions, 0% = On exchange quench control and 100% is fully deuterated and N = deuterium level measured before correction.

Deuterium that has been incorporated into the amides of an intact protein is rapidly lost from the very rapidly exchanging amino terminus proton and most N-terminal amide proton of peptides created under exchange quench conditions. Thus in our experiments, no hydrogen exchange information is available for the first two amino acids of a probe peptide. We use the term region to represent all amides where we can track deuterium incorporation. In some cases we specifically state the peptide identity as shown by mass spectrometry and label those as peptides (14,16). Regions of exchange were calculated by subtracting overlapping peptide

fragments as in previous work (22). Percent changes reported are calculated by the difference in exchange between conditions over the total number of deuterons in a region.

Results

Protein Digestion of GIA PLA_2

GIA PLA_2 is a very rigid protein due to its small size (13,500 kD) and the presence of seven disulfide bonds. Because of this, finding conditions for digesting the protein was a major hurdle to obtaining a good peptide map. TCEP has been employed to reduce disulfide bonds under the low pH conditions needed for deuterium exchange quenching (19). In our initial experiments, we added TCEP under a variety of conditions to the chromatographic solvents employed with the pepsin column in the automated DXMS system. This met with no success. We found that significant digestion could only be achieved by predigesting the enzyme with pepsin and fungal XIII protease prior to loading the samples onto the automated DXMS system described in the methods. The predigestion was achieved by quenching protein samples in a solution containing 1M TCEP and 8M GdHCl for 15 min followed by dilution into a solution containing immobilized pepsin and fungal XIII proteases for 15 min. This solution was then loaded onto the automated DXMS system and run through another immobilized pepsin column before being loaded onto the C18 column. Back exchange levels of ~50% were found with this technique, but by using fully deuterated controls, the amount of back exchange could be measured and used to determine corrected deuterium levels.

Using these conditions 55 good quality peptides were identified. If peptides occurred in more than one charge state, we have shown only the one with the best signal to noise ratio. This reduced the number of useful ions with no redundant data to 45, which are shown in Figure 1. This map covers 96% of the protein and has a high degree of overlap allowing for the determination of deuterium levels for regions of the protein smaller than the corresponding peptide. The difference in deuterium levels of the two overlapping peptides is the number of deuterons associated with the unmatched amino acids. This allows us to determine the deuteration levels of regions of the protein smaller than either peptide.

This map was generated in the presence of both metal ions and lipid without any changes in the number and intensity of peptide fragments. The number of deuterons incorporated was measured for all 55 peptides including peptides with multiple charge states, but to simplify the graphics only 23 of the peptides, those shown in bold lines in figure 1, were chosen to generate the deuterium exchange data for all of the other figures. However all 55 peptides were analyzed in each experiment to make sure that the exchange data agreed with that of the 21 selected peptides.

Deuterium Exchange of GIA PLA_2

On exchange experiments were carried out on the native GIA PLA_2 employing the DXMS methods outlined above. Figure 2 show deuterium exchange percentages for these experiments. Figure 2 is divided into 17 different regions. The deuterium levels of each region were generated by analyzing several overlapping peptides that allowed us to measure the deuteration level of the smallest protein regions possible.

The data show that both the N and C terminal regions (1-23, 102-119) of the protein exchange very rapidly (Fig 2). The first 23 amino acids encompass the first α helix and show over 80% deuteration within the first minute of on exchange with the exception of amino acids 9-10. Region 9-10 exchanges much slower and does not reach 80% deuteration until 60 min. This region encompasses the last two residues of the first α helix and is next to the disulfide bond bridging residues 11 and 71 as shown in Figure 3. This may explain the decreased rate of

exchange. The C terminal area stretching from amino acid 102-119 also shows over 80% deuteration within the first min of on exchange.

The region encompassing amino acids 56-86, which contains the two antiparallel β sheets, also shows very rapid exchange with deuteration rates comparable to those seen in both the N and C termini. The region from residue 24-40 is less flexible than the N and C termini and takes 60 min to fully exchange. In contrast, the rates of exchange on α helices 39-55 and 84-101 are very slow. The region from 89-101 exchanges less than 10% even after 24 hrs of on exchange. The region from 43-53 does exchange but only exchanges 50% after 4 hrs.

Changes in Deuterium Exchange of GIA PLA_2 when Ba^{2+} or Ca^{2+} is Bound

The GIA PLA_2 requires Ca^{2+} for activity with one molecule binding in the catalytic site. A second Ca^{2+} may also bind to the enzyme, but its role in activity has not been defined. Ba^{2+} also binds to the primary Ca^{2+} binding site in the catalytic site but it inhibits activity although it does produce similar structural changes in the enzyme as detected by UV-Vis spectroscopy (23). Thus, we measured deuterium on exchange of the GIA PLA_2 from 15 sec to 4 hrs in the presence of 1 mM $BaCl_2$ or $CaCl_2$ to ascertain if these metals produce different exchange patterns. Several areas in GIA PLA_2 show changes in deuterium exchange in the presence of Ca^{2+}. Three of these, 24-27, 29-40, 43-53 (Fig 4) are part of the primary Ca^{2+} -binding site of the GIA PLA_2 which consists of the backbone oxygens of Y27, G29, and G31 and the aspartic acid oxygens of D48 (10). Thus Ca^{2+} binding appears to decrease the deuterium exchange seen in regions 24-27, 29-40, and 43-53. Interestingly the decrease in deuterium exchange in regions 29-40 and 43-50 appears to mainly affect slow exchanging amide hydrogens. This is shown by the greatest difference in deuterium exchange being seen from 3,000-10,000 seconds (Fig 4).

One other region is 103-114 where the changes affect only fast exchanging amide hydrogens with no difference seen after 60 minutes of on-exchange. Since these residues are not part of the primary Ca^{2+} binding site, these results would be consistent with a second Ca^{2+} binding site. The crystal structures of the structurally related *N. naja atra* GIA PLA_2 have shown such a secondary Ca^{2+}-binding site with contacts between Asn 112, and Asp 23 and a secondary Ca^{2+} ion (24). By comparing the structures of these two enzymes, which are superimposable in this region, and overlaying the exchange data, it is clear that a Ca^{2+} binding to this second site in the *N. naja naja* PLA_2 would account for the exchange data (Fig 5).

The rates of exchange with $Ba^{2+}$are essentially the same for regions 29-40, 111-114, and 43-53. Ba^{2+} also causes changes in residues 103-110, and 24-27 although the magnitude of these changes is not as great as with Ca^{2+}.

These changes in exchange obviously have important structural implications because Ba^{2+} seems to bind the same sites, but in such a way as to inactivate the enzyme. These results are consistent with a picture in which Ba^{2+} binds competitively for the Ca^{2+} -binding site. The affinity of Ba^{2+} and Ca^{2+} is different with K_d values of 0.15 mM and 0.4 mM, respectively (23), and these differences in affinity may explain the difference in exchange seen at the Ca^{2+} binding sites.

Deuterium Exchange of GIA PLA_2 in the Presence of Lipid

One of the main goals of this research was to determine if deuterium exchange could yield information about how the soluble GIA PLA_2 interacts with large substrate aggregates. To that end deuterium exchange of GIA PLA_2 at time points varying from 15 sec to 1 hr was analyzed in the presence of 1mM small unilamellar vesicles (SUVs) of DPPC. These experiments were carried out in the absence of Ca^{2+} to prevent hydrolysis of the phospholipid vesicles. EDTA

was included to insure that no free Ca^{2+} was present. Previous work in our lab has shown very low levels of enzyme binding to phospholipid without metal present, but that either Ca^{+2} or Ba^{+2} increased this level of phospholipid binding (25). For this reason experiments were also carried out using Ba^{2+} (data not shown) as a replacement for Ca^{2+}, which achieved the exact same exchange patterns as with lipid in the absence of metal ions. Studies were done at 22 °C because it has been shown that the GIA PLA_2 has a significant lag phase with lipid above the phase transition temperature (26), so we desired our lipid surface to be only in the gel state. Most regions of the GIA PLA_2 show no change in deuterium exchange in the presence of DPPC lipid vesicles, except for one small region of the protein. This area is amino acids Ile9, and Lys10 (Fig. 6). The deuteration level of region 9-10 was calculated by subtracting the deuterium levels of peptide 1-8 from 1-10; the same decrease in exchange with lipid is seen in 5 other peptides (1-17,1-21,1-27,5-21,5-27) that include region 9-10. This effect is not seen in peptides 9-21, 9-17, 11-21, and 9-27 which do not include region 9-10 (noting that the first two amino acids fully exchange with the technique and are not included in the analysis). This shows that the effect is strictly limited to the region 9-10. There is a 20-30% change between the lipid free and DPPC containing protein samples.

Further experiments were done using 100 μM Ca^{2+} with phospholipid vesicles to minimally activate the enzyme. Original experiments using DPPC vesicles with 100 μM Ca^{2+} at 22 °C caused high levels of phospholipid hydrolysis. Further experiments were done at 0 °C to further slow hydrolysis so total phospholipid hydrolysis stayed below 10% over the deuterium on exchange time course. Due to the change in temperature, the lipid used was shifted from DPPC to DMPC. The phase transition temperatures of DPPC and DMPC are 41 and 23 respectively, so we used DMPC at 0 °C to view a similar physical state of the lipid as DPPC studies at 22 °C. Activity assays performed showed that at 300 seconds the enzyme had not hydrolyzed more then 10% of the lipid surface. Four regions of the protein, namely regions 3-5, 6-8, 18-21, and 56-64, had significant decreases in exchange upon exposure to lipid in the presence of calcium (Fig. 7). Deuterium content for region 6-8 was calculated through subtraction of peptides 1-5 from 1-8, and deuterium content of region 18-21 was calculated through subtraction of peptides 1-17, from 1-21.

Regions 3-5, and 6-8 are part of the first alpha helix located on the i-face of the enzyme. Due to multiple overlapping peptides in this region we were able to localize changes in this helix. The largest change was seen from region 3-5 containing Tyr-3, and Phe-5 and had a 20-30% decrease in exchange over all timepoints. Interestingly from using peptide overlap data from peptide 1-4 and peptide 1-5, it seems that both amino acids 3-4 and amino acid 5 have independent decreases in exchange. Region 3-4 had a smaller decrease in exchange at 100 and 300 seconds, with residue 5 having a constant deuterium decrease. Region 6-8 also had a 10-20% decrease in exchange. The region 18-21 had a 5-10% decrease in exchange, and it contains Trp-18, and Trp-19. Region 56-64 had a 10-20% decrease in exchange until 100 seconds, with less then 10% at 300 seconds. The region 9-10 which had a decrease in exchange with lipid and no Ca^{2+} present at 22 °C (Fig 6) had zero on exchange at 0 °C up to 300 seconds, so no change could be detected with lipid in the presence of Ca^{2+} at these lower temperatures. Importantly, this experiment shows interaction of phospholipid with the i-face of the protein and demonstrates the potential of deuterium exchange mass spectrometry to study proteins that catalyze reactions at the lipid surface.

Discussion

There are many crystal structures of GIA PLA_2, but these structures only show a static picture of the enzyme under crystallization conditions. Using deuterium exchange mass spectrometry, we are able to study the protein in solution under varying conditions. This represents the first use of deuterium exchange mass spectrometry to probe the structure of a PLA_2 and its

interaction with a lipid surface. In the present study, we show a region of the protein that is solvent accessible blocked from exchange by extensive disulfide bonds, the presence of a secondary Ca^{2+} binding site in the *N. naja naja* GIA PLA_2 as well as showing the ability to probe lipid-lipase interactions with deuterium exchange mass spectrometry.

The on exchange experiments on the native GIA PLA_2 showed that the three α-helices exhibited dramatically different exchange rates. The N-terminal helix exchanges vary rapidly while the two core helices exhibit almost no exchange even though they are on the surface of the protein and at least some of the amide protons should be accessible to water. The difference is that helices 39 to 55 and 84-101 are involved in four disulfide bonds with other parts of the protein while the N-terminus is not. Other regions that are not involved in extensive disulfide bonding also show very fast deuterium exchange rates as would be expected for such a small solvent exposed protein. Studies performed on a recombinant macrophage colony stimulating factor-beta with nine disulfide bonds (6 intramolecular and 3 intermolecular), did not reveal this same lack of deuterium exchange in surface exposed disulfide bonding areas (19). That study concluded that exchange rates were mainly due to solvent accessibility. The exchange rates of α helices in this protein were correlated to depth from solvent rather then conformational constraints from disulfide bonds. This protein is a dimer of two 221 amino acid subunits that is quite large and contains 9 disulfide bonds. The difference in the exchange rates between this protein and GIA PLA_2 is because of the higher percentage of disulfide bonds in this protein and the localization of these bonds intertwined with the two α helices. The amino acids participating in disulfide bonds are shown in figure 3 with six of the cysteine residues located on the two helices. This is a novel finding as it has not been previously demonstrated that extensively disulfide bonded areas of proteins are held extremely rigidly by those bonds and that exchange with the solvent is restricted.

Because of this tight disulfide bond structure the protein is very resistant to both digestion and denaturation and needed extreme conditions to fragment the protein. This extremely tight disulfide bonded network is a possible evolutionary adjustment in toxin containing PLA_2s to protect against protease digestion in the venom or in their prey. Our use of a pre-digestion with TCEP was necessary to achieve these results and provides a procedure to now investigate other highly disulfide bonded proteins.

Two crystal structures of the *N. naja naja* GIA PLA_2 have been previously solved by our laboratory (6,10). In both of these crystals, the enzyme was present as trimers. The *N. naja atra* GIA PLA_2 structure was solved as a dimer and contained two Ca^{2+} -binding sites per enzyme molecule (24). The structure of *N. naja naja* (10) by Fremont et al. contained Ca^{2+} in the primary binding site, but did not show this secondary Ca^{2+}. However the trimer structure is held together by an intermolecular salt bridge between Arg30 on one monomer and Asp23 on a second monomer. Asp23 is one of the essential residues in binding the secondary Ca^{2+} as shown in the *N. naja atra* crystal. This trimer interaction occurs at high enzyme concentrations and may block the incorporation of the secondary Ca^{2+} ion. We could not isolate Asp23 in the DXMS analysis because of the lack of overlap of peptides in this region.

The C terminal region from 103-114 also forms part of the secondary site. This region does show a decrease in exchange that would suggest the presence of Ca^{2+} in this site. This indicates that when the enzyme is in solution, Ca^{2+} is bound to the second site, and that the lack of the second Ca^{2+} in the original crystal structure was due to the trimer contacts with Asp23. If a model is generated with the *N. naja naja* crystal structure containing a Ca^{2+} ion in the secondary Ca^{2+} binding site shown in the *N. naja atra* structure, the amino acids are in the correct position for Ca^{2+} binding.

Ba^{2+} showed decreases in deuterium exchange as did Ca^{2+}, but the magnitude of the change was less. Decreases in deuterium exchange at the Ca^{2+} binding sites were lower in the presence of Ba^{2+} then at the same levels of Ca^{2+}. This is most likely due to the different affinities of these ions for the enzyme of 0.15 mM for Ca^{2+} and 0.4 mM for Ba^{2+} (23). These results suggest that Ba^{2+} binds in exactly the same place as the Ca^{2+} ion, but there are differences in the affinity at the site of binding.

The interfacial activation of PLA_2 has been an area of interest for many years. The use of DPPC vesicles, without Ca^{2+} present to probe lipid binding did not show changes in deuterium exchange in large areas of the protein. However there was a distinct effect in residues 9-10. This region contains isoleucine 9, which has been postulated to be one of the residues in the hydrophobic core in the active site of the protein based on the crystal structure (24,27). This change in deuterium exchange may well be the interaction of the sn-2 fatty acid from the phospholipid with the hydrophobic residue.

Experiments caried out in the presence of low levels of Ca^{2+} with DMPC SUVs showed significant decreases in exchange in large areas of the enzyme proposed to bind the membrane interface. A hypothetical scheme of membrane binding of the GIA N. *naja naja* PLA_2 is shown in Fig. 8.

Our experiments showed decreases in exchange at regions containing Tyr-3, Trp-61, Tyr-63. and Phe-64. We propose that the aromatic residues here are inserting into the membrane bilayer. Mutations of the aromatic amino acids have been tested in the structurally similar N. naja atra GIA PLA_2 enzyme and found to significantly diminish interfacial activation (28). Similar experiments in the N. *naja naja* GIA enzyme showed mutations at Trp-61, Tyr-63, and Phe-64 also significantly reduced interfacial inactivation (8). Our experiments also show a decrease in region 6-8 containing Lys-6, which is in the correct orientation to interact with phosphate headgroups of the membrane surface. Experiments using the GIA PLA_2 inhibitor manoalide showed that reaction of manoalide with Lys-6 caused a large decrease in activity, maybe inducing an incorrect protein orientation at the surface (29). The deuterium exchange data suggests that the majority of the interactions between the enzyme and the interface are mediated by regions 3-8, and 56-64. The area 18-21 has a very small change in exchange compared to changes seen from 3-8 and 56-64. We propose that binding to a lipid surface is mediated by the aromatic and charged residues in these areas and blocks them from solvent exposure. Our experiments confirm that these areas of the enzyme are interacting with the membrane surface, but only upon exposure to Ca^{2+}.

Our experiments also demonstrate a decrease at regions containing Phe-5, Ile-9, and Trp-19. We propose these amino acids are mediating binding of the fatty acyl tails of phospholipid substrate. Previous NMR studies carried out by our laboratory using an amide substrate analogue dispersed in micelles showed differences in Leu-2, Phe-5, Trp-19, Ala-22, and Phe 100 with GIA PLA_2 (12). There also exists a crystal structure of the *N. naja atra* enzyme with an inhibitor bound showing hydrophobic interactions between Leu-2, Phe-5, Ile-9, Trp-19, and Tyr-69 (27). Our deuterium exchange results very closely match the results seen in both inhibitor bound GIA PLA_2's. In our studies we were not able to isolate Leu-2, Ala-22, or Phe-100 due to very slow exchange in these regions, or lack of resolution. The changes seen at Ile-9, and Phe-5 have a constant level of decrease in exchange at all timepoints, where regions proposed to penetrate the membrane surface have smaller decreases in exchange at later timepoints. This suggests that substrate binds very tightly and blocks this area from on exchange at all timepoints, while the enzyme may hop on and off substrate, allowing surface penetrating residues to exchange at later timepoints.

Conclusion

This study shows rigidification of the two extensively disulfide bonded helices, and the presence of a secondary Ca^{2+} binding site present in the N. *naja naja* group Group IA PLA_2. Also we have shown that both of these sites show changes upon Ba^{2+} binding, but not at the same levels of exchange. This study also shows an interaction between the soluble enzyme and the lipid surface at both surface and substrate binding regions of the protein. This study marks a novel use of deuterium exchange mass spectrometry to study lipid-lipase interactions, as well as using novel digestion and denaturation methods to work with very highly disulfide bonded proteins.

Acknowledgements

The authors are extremely grateful to Dr (Howard) Yuan-Hao Hsu for critical discussions of this work.

This work was supported by NIH Grants GM 20501 (EAD) and CA 099835, CA 118595, and AI 076961 (VLW).

Reference List

1. Six DA, Dennis EA. The Expanding Superfamily of Phospholipase A_2 Enzymes: Classification and Characterization. Biochim Biophys Acta 2000;1488:1–19. [PubMed: 11080672]
2. Schaloske RH, Dennis EA. The Phospholipase A_2 Superfamily And Its Group Numbering System. Biochim Biophys Acta 2006;1761:1246–1259. [PubMed: 16973413]
3. Balsinde J, Balboa MA, Insel PA, Dennis EA. Regulation and Inhibition of Phospholipase A_2. Ann Reviews of Pharmacology and Toxicology 1999;39:175–189.
4. Plückthun A, Rohlfs R, Davidson FF, Dennis EA. Short-Chain Phosphatidylethanolamines: Physical Properties and Susceptibility of the Monomers to Phospholipase A_2 Action. Biochemistry 1985;24:4201–4208. [PubMed: 4052390]
5. Adamich M, Roberts MF, Dennis EA. Phospholipid Activation of Cobra Venom Phospholipase A_2. II. Characterization of the Phospholipid-Enzyme Interaction. Biochemistry 1979;18:3308–3313. [PubMed: 465469]
6. Segelke BW, Nguyen D, Chee R, Xuong NH, Dennis EA. Structures of Two Novel Crystal Forms of *Naja naja naja* Phospholipase A_2 Lacking Ca^{2+} Reveal Trimeric Packing. J Mol Biol 1998;279:223–232. [PubMed: 9636712]
7. Ortiz AR, Pisabarro MT, Gallego J, Gago F. Implications of a consensus recognition site for phosphatidylcholine separate from the active site in cobra venom phospholipases A_2. Biochemistry 1992;31:2887–2896. [PubMed: 1550815]
8. Lefkowitz LJ, Deems RA, Dennis EA. Expression of Group IA Phospholipase A_2 in *Pichia pastoris*: Identification of a Phosphatidylcholine Activator Site Using Site-Directed Mutagenesis. Biochemistry 1999;38(43):14174–14184. [PubMed: 10571991]
9. Deems RA, Eaton BR, Dennis EA. Kinetic Analysis of Phospholipase A_2 Activity Toward Mixed Micelles and Its Implications for the Study of Lipolytic Enzymes. Journal of Biological Chemistry 1975;250:9013–9020. [PubMed: 1194274]
10. Fremont DH, Anderson D, Wilson IA, Dennis EA, Xuong NH. The Crystal Structure of Phospholipase A_2 from Indian Cobra Reveals a Novel Trimeric Association. Proc Natl Acad Sci U S A 1993;90:342–346. [PubMed: 8419939]
11. Plesniak LA, Boegeman SC, Segelke BW, Dennis EA. Interaction of Phospholipase A_2 with Thioether Amide Containing Phospholipid Analogues. Biochemistry 1993;32:5009–5016. [PubMed: 8494876]
12. Plesniak L, Yu L, Dennis EA. Conformation of Micellar Phospholipid Bound to the Active Site of Phospholipase A_2. Biochemistry 1995;34:4943–4951. [PubMed: 7711016]
13. Mandell JG, Falick AM, Komives EA. Identification of protein-protein interfaces by decreased amide proton solvent accessibility. Proc Natl Acad Sci U S A 1998;95:14705–14710. [PubMed: 9843953]
14. Hamuro Y, Anand GS, Kim JS, Juliano C, Stranz DD, Taylor SS, Woods VL Jr. Mapping intersubunit interactions of the regulatory subunit (RIalpha) in the type I holoenzyme of protein kinase A by amide

hydrogen/deuterium exchange mass spectrometry (DXMS). J Mol Biol 2004;340:1185–1196. [PubMed: 15236976]

15. Hoofnagle AN, Resing KA, Goldsmith EJ, Ahn NG. Changes in protein conformational mobility upon activation of extracellular regulated protein kinase-2 as detected by hydrogen exchange. Proc Natl Acad Sci U S A 2001;98:956–961. [PubMed: 11158577]
16. Brudler R, Gessner CR, Li S, Tyndall S, Getzoff ED, Woods VL Jr. PAS domain allostery and light-induced conformational changes in photoactive yellow protein upon I2 intermediate formation, probed with enhanced hydrogen/deuterium exchange mass spectrometry. J Mol Biol 2006;363:148–160. [PubMed: 16952373]
17. Wales TE, Engen JR. Hydrogen exchange mass spectrometry for the analysis of protein dynamics. Mass Spectrom Rev 2006;25:158–170. [PubMed: 16208684]
18. Man P, Montagner C, Vernier G, Dublet B, Chenal A, Forest E, Forge V. Defining the interacting regions between apomyoglobin and lipid membrane by hydrogen/deuterium exchange coupled to mass spectrometry. J Mol Biol 2007;368:464–472. [PubMed: 17346745]
19. Yan X, Zhang H, Watson J, Schimerlik MI, Deinzer ML. Hydrogen/deuterium exchange and mass spectrometric analysis of a protein containing multiple disulfide bonds: Solution structure of recombinant macrophage colony stimulating factor-beta (rhM-CSFbeta). Protein Sci 2002;11:2113–2124. [PubMed: 12192067]
20. Hazlett TL, Dennis EA. Affinity Chromatography of Phospholipase A_2 from *N. naja naja* (Indian Cobra) Venom. Toxicon 1985;23:457–466. [PubMed: 3927524]
21. Zhang Z, Smith DL. Determination of amide hydrogen exchange by mass spectrometry: a new tool for protein structure elucidation. Protein Sci 1993;2:522–531. [PubMed: 8390883]
22. Del Mar C, Greenbaum EA, Mayne L, Englander SW, Woods VL Jr. Structure and properties of alpha-synuclein and other amyloids determined at the amino acid level. Proc Natl Acad Sci U S A 2005;102:15477–15482. [PubMed: 16223878]
23. Roberts MF, Deems RA, Dennis EA. Spectral Perturbations of the Histidine and Tryptophan in Cobra Venom Phospholipase A_2 Upon Metal Ion and Mixed Micelle Binding. Journal of Biological Chemistry 1977;252:6011–6017. [PubMed: 19461]
24. Scott DL, White SP, Otwinowski Z, Yuan W, Gelb MH, Sigler PB. Interfacial catalysis: the mechanism of phospholipase A2. Science 1990;250:1541–1546. [PubMed: 2274785]
25. Roberts MF, Deems RA, Dennis EA. Dual Role of Interfacial Phospholipid in Phospholipase A_2 Catalysis. Proc Natl Acad Sci U S A 1977;74:1950–1954. [PubMed: 266715]
26. Kensil CR, Dennis EA. Action of Cobra Venom Phospholipase A_2 on the Gel and Liquid Crystalline States of Dimyristoyl and Dipalmitoyl Phosphatidylcholine Vesicles. Journal of Biological Chemistry 1979;254:5843–5848. [PubMed: 582173]
27. White SP, Scott DL, Otwinowski Z, Gelb MH, Sigler PB. Crystal structure of cobra-venom phospholipase A2 in a complex with a transition-state analogue. Science 1990;250:1560–1563. [PubMed: 2274787]
28. Stahelin RV, Cho W. Differential roles of ionic, aliphatic, and aromatic residues in membrane-protein interactions: a surface plasmon resonance study on phospholipases A2. Biochemistry 2001;40:4672–4678. [PubMed: 11294634]
29. Ghomashchi F, Yu BZ, Mihelich ED, Jain MK, Gelb MH. Kinetic characterization of phospholipase A2 modified by manoalogue. Biochemistry 1991;30:9559–9569. [PubMed: 1911741]

Abbreviations

GIA PLA_2
: Group IA Phospholipase A_2

DXMS
: Deuterium exchange mass spectrometry

DMPC
: dimyristoyl phosphatidylcholine

DPPC

dipalmitoyl phosphatidylcholine

GdHCl

Guanidine Hydrochloride

TCEP

Tris-carboxy ethyl phosphine

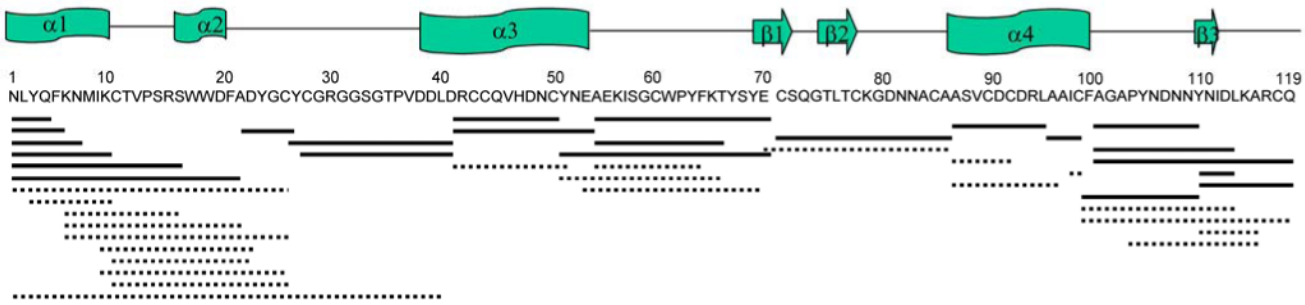

Figure 1.

Pepsin digested peptide coverage map of the GIA PLA_2 sequence with alpha helical (α) and beta sheet (β) regions indicated. Black lines represent peptides chosen for this study. Dotted lines represent peptides that were identified and analyzed but were only used as a comparison for the bold line peptides. There are 45 distinct peptides which were studied with only one selected for peptides that have multiple charge states.

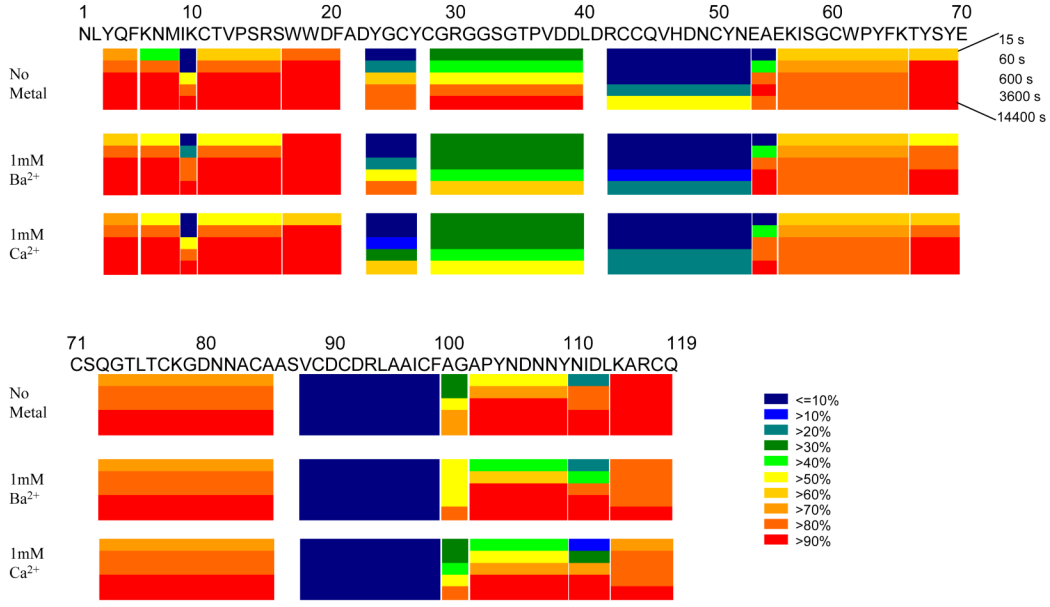

Fig. 2.

Amide hydrogen/deuterium exchange analysis of the calcium and barium effect on GIA PLA_2. The deuterium exchange map with and without Ba^{2+} and Ca^{2+} is shown with the amino acid sequence of the GIA PLA_2. Each condition is divided into rows corresponding to each time point, from 15s to 240 min from top to bottom. The colors code for the amount of H/D exchange in the given time period.

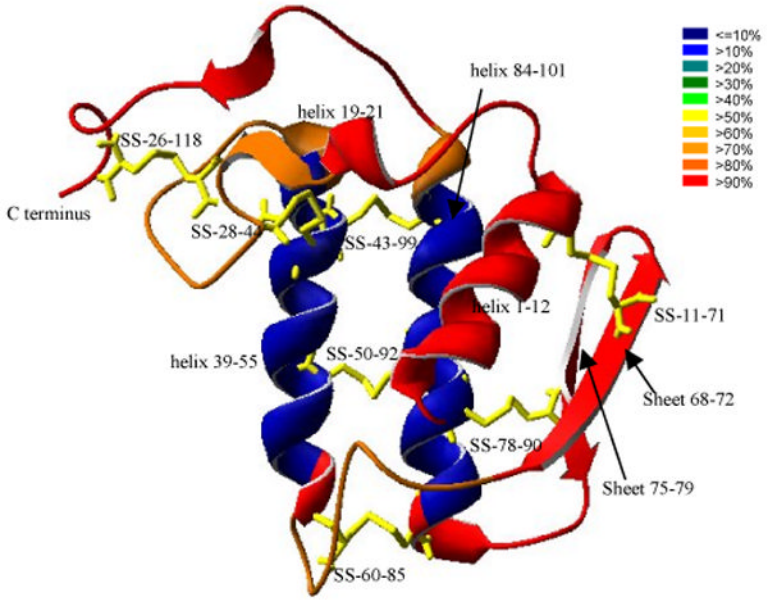

Fig. 3.

Deuteration level of GIVA PLA_2 visualized on the crystallographic model of the *N. naja naja* enzyme (1PSH). The deuterium exchange map of GIVA PLA_2 after 3000 seconds of on-exchange is shown with the color indicating the exchange rates detected by DXMS. Disulfide bonds are shown in yellow.

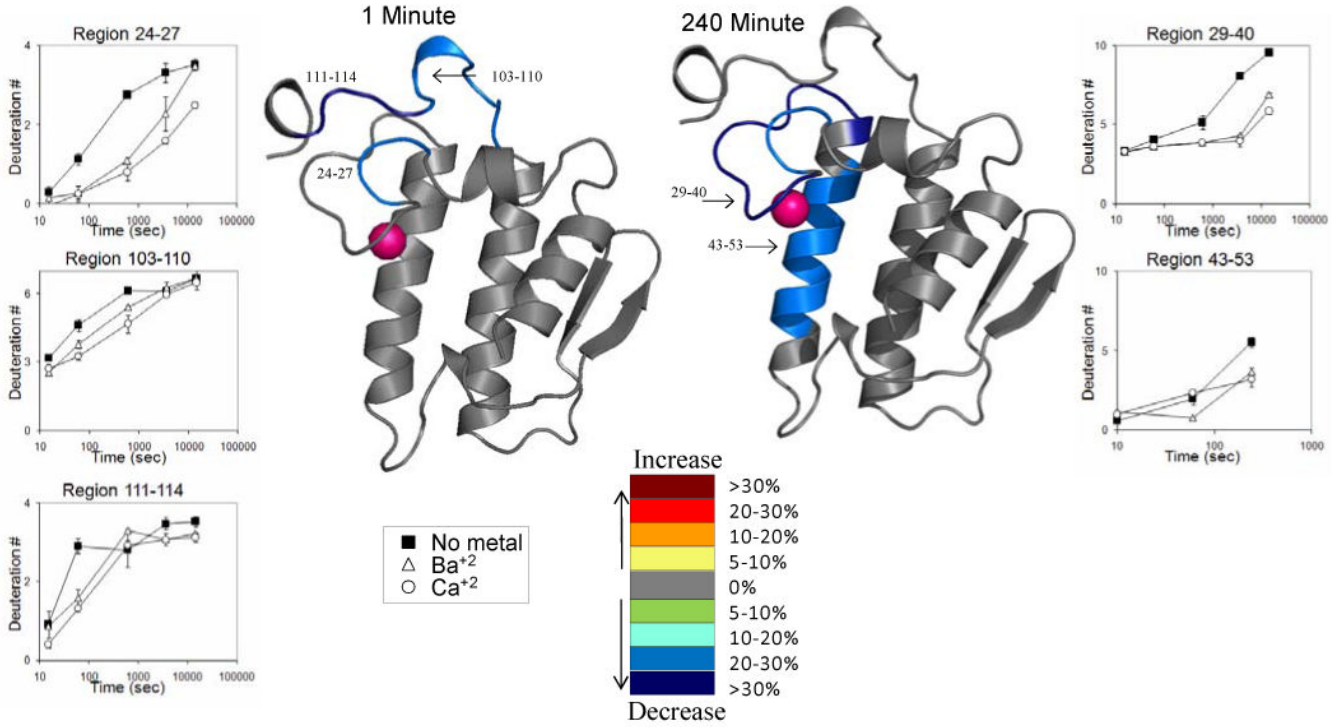

Fig. 4.

Deuterium exchange of the GIA PLA_2 upon metal binding. The number of incorporated deuterons at 5 time points are plotted for regions that show changes upon either calcium or barium (or both) binding. The changes in deuterium exchange are shown at two different time points mapped on the *N. naja naja* GIA PLA_2 crystal structure (1PSH) with the calcium ion shown in pink. The color represents the changes in deuterium levels.

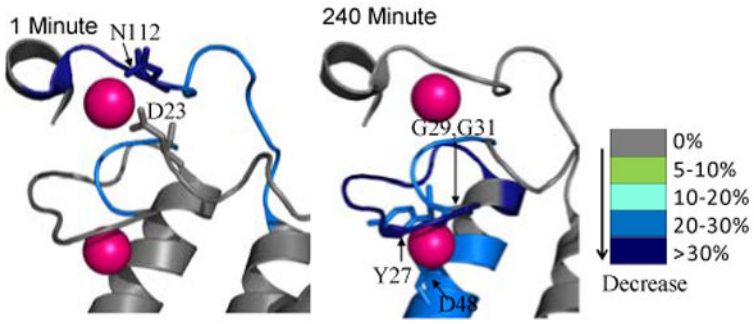

Fig. 5.

Crystal structure of the *N. naja atra* GIA PLA_2 with a secondary calcium site present and the calcium ions shown in pink. The deuterium exchange data from *N. naja naja* PLA_2 was overlaid onto the *N. naja atra* structure (1POA) for two time points. Amino acids involved in binding the calcium ions are labeled. The color represents the change in deuterium levels.

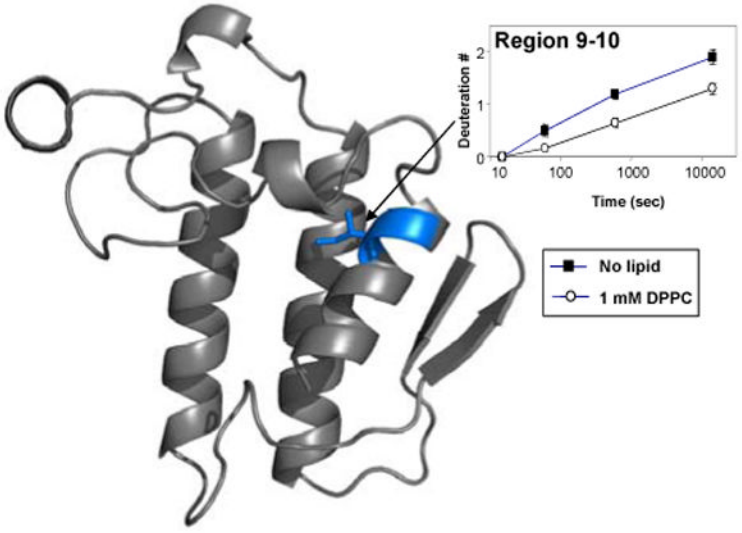

Fig. 6.

Deuterium exchange of the GIA PLA_2 with areas of decreased exchange upon phospholipid binding in the presence of 1 mM EDTA. The number of incorporated deuterons at four time points is plotted for region 9-10. Changes were mapped onto the *N. naja naja* GIA PLA_2 crystal structure (1A3D).

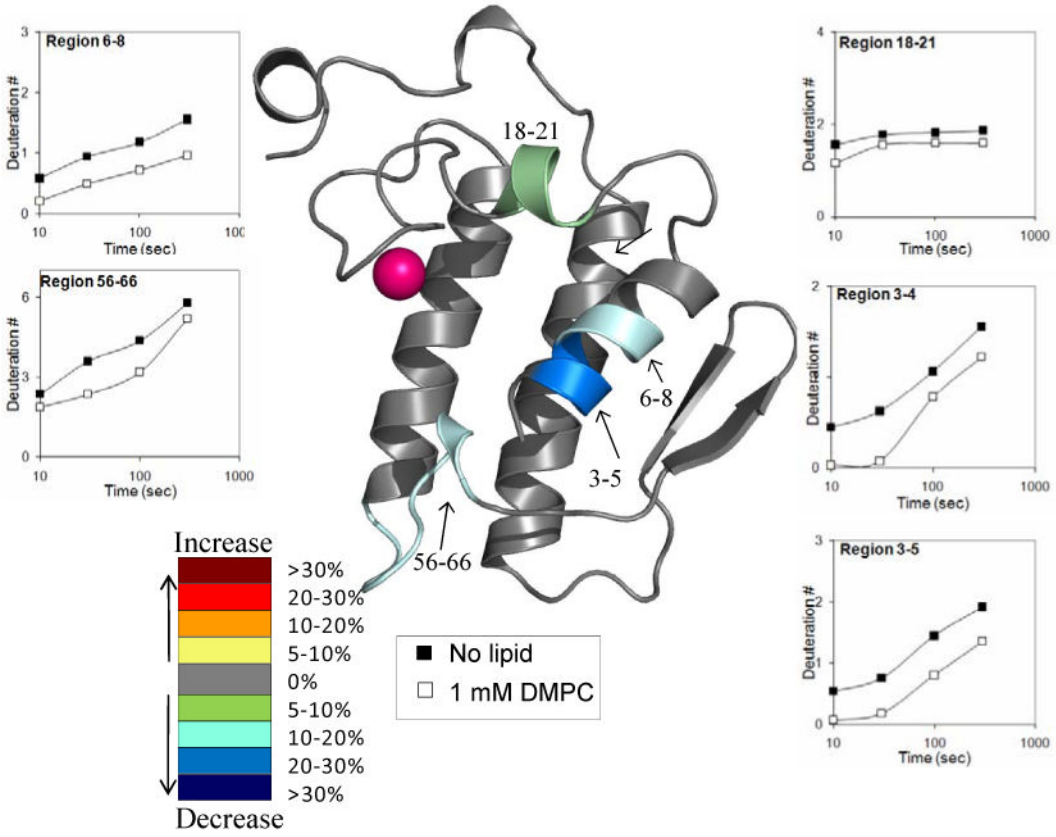

Fig. 7.

Deuterium exchange of the GIA PLA_2 upon DMPC vesicle binding at 0 °C in the presence of 100 μM Ca^{2+}. The number of incorporated deuterons at 4 time points are plotted for regions that show changes upon DMPC binding. The changes in deuterium exchange are shown mapped on the *N. naja naja* GIA PLA_2 crystal structure (1PSH) with the calcium ion shown in pink. The color represents the changes in deuterium levels.

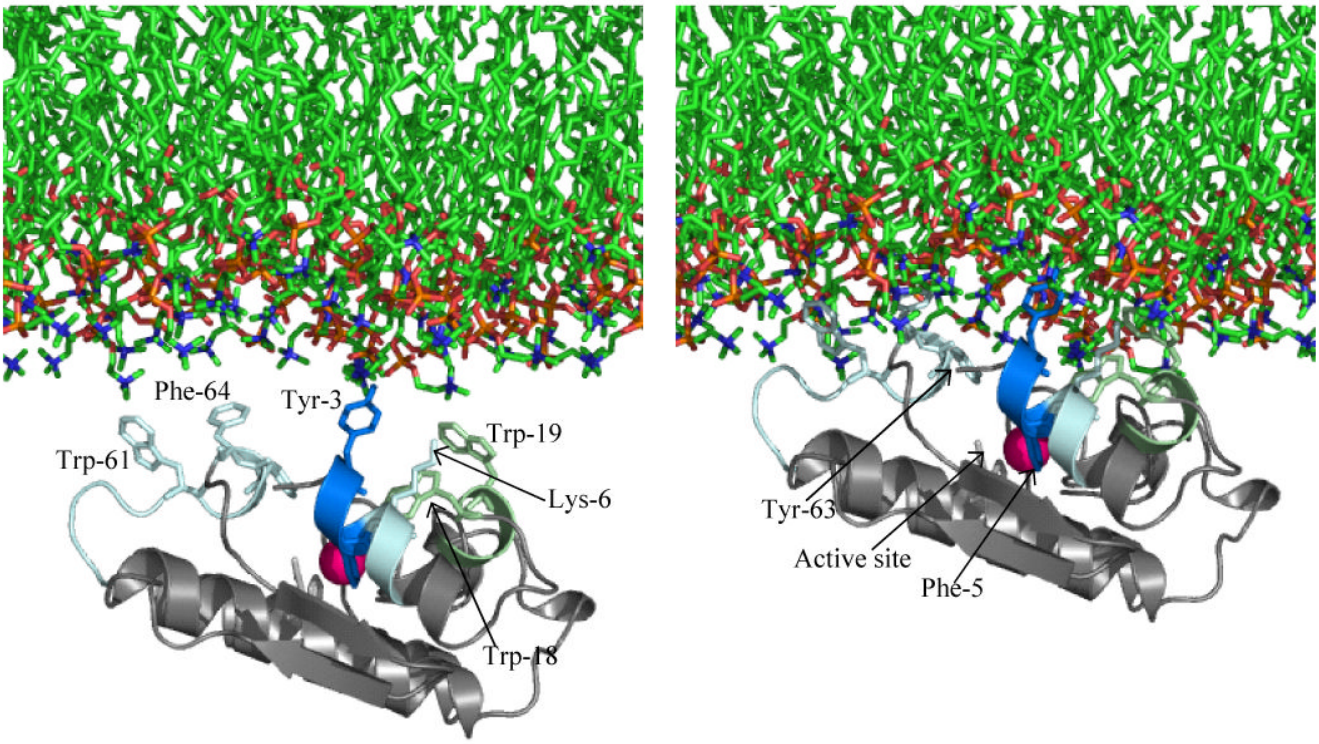

Figure 8.

Hypothetical model of GIA PLA_2 binding to a DMPC membrane surface (left) before associating with the membrane and (right) after association with the membrane. Areas with decreases in exchange have been colored and amino acid residues Tyr-3, Phe-5, Lys-6, Trp-18, Trp-19, His-47, Trp-61, Tyr-63, Phe-64, and Asp-93 have been drawn in stick form. Figure was created in PyMol.